A Study of Signatures of Revivals and Fractional Revivals in an Optical Tomogram

Bhutekar Vishal Ganeshrao
Research Student

Introduction:

Optical tomography will be used to provide additional spatially resolved information to the research team. Following the application of light, the distribution of photons inside the specimen is reconstructed. Turbid and dense media are examples of media that have difficulty with light distribution, which is why the transillumination-based approach to 3D OI is referred to as diffuse optical tomography (DOT).

The acquisition of signals (from above) and known coordinates (for example, for the application of light or photons used for excitation) is needed in order to recover all data naturally; in the light of fluorescence tomography, the acquisition of the origin of an evoked photon is also necessary (fluorescence imaging). This necessitates the development of a reconstruction technique, and much effort has been devoted to improving the accuracy of photon distribution forecasts in turbid media/tissue, independent of the scanning technology used.

Mismatches between measured and applied intensities, as well as the determination of the true intensity of a fluorescent source inside tissue, provide major challenges in optical image reconstruction. Progress in computer technology over the preceding decade, which enabled computers to handle more complex mathematical processes while also making more accurate assumptions about the optical properties of the specimen, made a significant contribution to the overall performance of 3D OI. Attempting to predict the quantity of light that a photon might scatter inside a tissue sample is referred to as the "forward problem" by more contemporary authors. The phrase "inverse issues" refers to the process of calculating how much light was dispersed by a photon in the opposite direction.

Analysis:

The optical tomogram for the time-changed state provided in Equation is calculated in this section and the signatures from revivals and split revivals are looked for directly in the optical tomogram. We remember the optical tomogram of the coherent state $|\alpha\rangle$, given by Eq., is a structure with a single sinusoidal strand in the X_θ-θ plane, and the maximum intensity of the optical tomogram along the X_θ axis occurs at $X_\theta = \sqrt{2|\alpha|^2}\cos\delta$. The quantity μ is the justification for the complex number α. The optical state tomogram at any moment in the development of a coherent state $|\alpha\rangle$ is calculated by substituting Eq.:

$$\omega(X_\theta,\theta,t)=\frac{\exp[-|\alpha|^2-X_\theta^2]}{\sqrt{\pi}}\left|\sum_{n=0}^{\infty}\frac{\alpha^n e^{-i\chi tn(n-1)}e^{-in\theta}H_n(X_\theta)}{n!\,2^n/2}\right|^2$$

In the following we analyze the optical tomogram ω (X_θ, θ, t) At fractional revivals instants. At a period of partial resurgence for k t = π/kχ, Eq. can be simplified to get the optical tomogram of the state $|\psi^{(k)}\rangle$ as

$$\omega^{(k)}(X_\theta,\theta)=\frac{1}{\sqrt{\pi}}\left|\sum_{s=0}^{k-1}f_{s,k}\exp\left\{\left[-\frac{X_\theta^2}{2}-\frac{|\alpha|^2}{2}-\frac{\alpha_s^2e^{-i2\theta}}{2}+\sqrt{2}\alpha_sX_\theta e^{-i\theta}\right]\right\}\right|^2$$

Where

$$f_{s,k}=\begin{cases}f_s & \text{if } k \text{ is odd}\\ g_s & \text{if } k \text{ is even,}\end{cases}$$

$$\alpha_s=\begin{cases}\alpha\, e^{-i\,2\pi s/k} & \text{if } k \text{ is odd}\\ \alpha\, e^{i\pi/k}\, e^{-i\,2\pi s/k} & \text{if } k \text{ is even.}\end{cases}$$

Figures 4.9(a)-4.9(c), show the optical tomograms of the state $|\omega^{(k)}\rangle$ for k = 2, 3, And 4, corresponds to the fractional revivals of both, three and four subpackage of the

original coherent state, respectively. The Field strength value $|\alpha|^2$ used to plot the tomograms is 20. The state $|\psi^{(2)}\rangle$ is a superposition of the coherent states $|\alpha\rangle$ and $|-\alpha\rangle$ with weights (1 − i)/2 and (1 + i)/2 (Eq. expansion coefficients of Fourier). The optical tomogram of this state is a two-stranded structure. Therefore, the structure with two sinusoidal strands in the time-evolved state optical tomogram for an initial coherent state $T_{rev}/2$ Is a two-subpack fractional revival signature. Note that the states' optical tomogram $|\psi^{(2)}\rangle$, shoWn in Fig. 4.9(a), is different from an even cohesive optical tomogram given in Fig. 4.9 (a). The highest intensity of the optical tomogram of the state along the X/axis $|\psi^{(2)}\rangle$ occur at locations $X_\theta = \sqrt{2|\alpha|^2}\, cos\,(\delta + \pi/2)$ and $X_\theta = \sqrt{2|\alpha|^2}\, cos\,(\delta + 3\pi/2)$, whereas, for an even coherent state, this occur at locations $X_\theta = \sqrt{2|\alpha|^2}\, cos\,(\delta)\; and\; X_\theta = \sqrt{2|\alpha|^2}\cos(\delta + \pi)$. In Fig. 4.9(a), the maximum intensity of the optical tomogram along the X_θ axis occur at $X_\theta = \sqrt{40}\cos(3\pi/4)$and $X_\theta = \sqrt{40}\cos(7\pi/4)$, corresponding to the sinusoidal strands of $|i\alpha\rangle$ and $|-i\alpha\rangle$, respectively. The quantum interference regions between the states $|i\alpha\rangle$ and $|-i\alpha\rangle$ are reflected in the optical tomogram of the state $|\psi^{(2)}\rangle$ at locations in the X_θ-θ Plane, where two sinusoidal strands cross and exhibit a big swing in the optical tomogram.

The optical tomogram of the state $|\psi^{(3)}\rangle$, The state at a fractional revival of the three subpackages, shown in Fig. 4.9(b), shows a structure with 3 sinusoidal strands. Similarly, the State optical tomogram $|\psi^{(4)}\rangle$, which is a state at the four-subpacket fractional revival, plotted in Fig. 4.9(c), shows a structure with four sinusoidal strands. The optical tomorams of the states $|\psi^{(3)}\rangle$ and $|\psi^{(4)}\rangle$ are different from the optical tomogram of the state $|\psi_{3,0}\rangle$ and $|\psi_{4,0}\rangle$ (For example, Figs. 4.4(a) and 4.4(b) correspondingly. We have performed the study for higher orders of fractional revivals (k > 4), and have established the general conclusion that a structure with k sinusoidal branches displays the optical tomogram of the developed state at the k subpacket of fractional revival time.

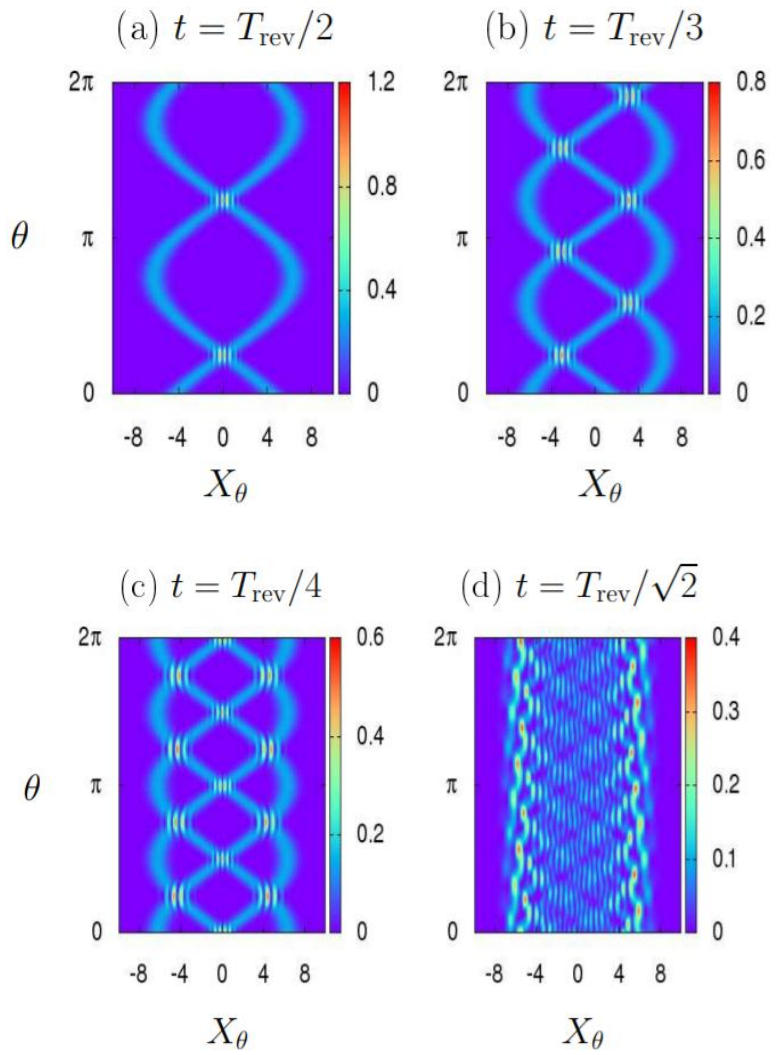

Figure 1- Time-evolved optical tomogram ω (X_θ, θ, t) for an initial coherent state |α⟩ with field strength $|\alpha|^2 = 20$ at times (a) $t = T_{rev}/2$, (b) $t = T_{rev}/3$, (c) $t = T_{rev}/4$, and (d) $t = T_{rev}/\sqrt{2}$. At a k-subpacket fractional revival time $t = \pi/k\chi$, the optical tomogram of the state shows structures with k sinusoidal strands. The structures with sinusoidal strands are completely absent in the optical tomogram for the collapsed state at time $t = T_{rev}/\sqrt{2}$

During the evolution of the coherent state $|\alpha\rangle$, the wave packet may also show the collapse phenomenon at specific instants of time $t = T_{rev}/s$, Where s is unreasonable. Where s is irrational. The collapse phenomena relates to the annihilation of a wave packet in a nonlinear medium during its development as a consequence of the destructive interference of wave packet states.

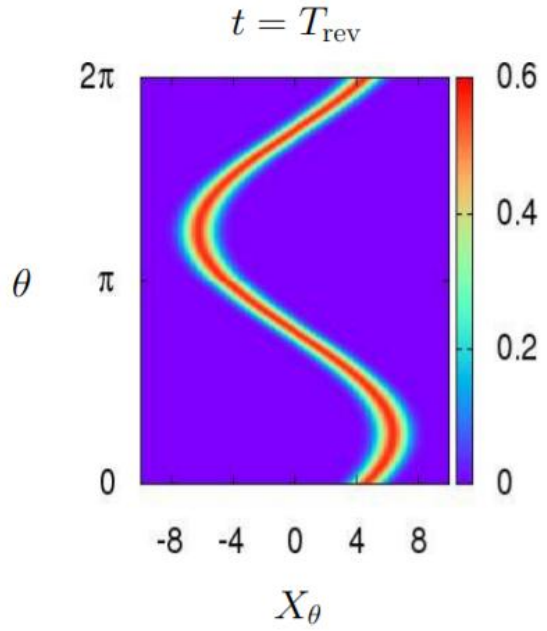

Figure 2 - Optical tomogram ω ($X_θ$, θ, t) for an initial coherent state $|\alpha\rangle$ with field strength $|\alpha|^2$ = 20 at revival time t = T_{rev}.

Conclusions:

The state is called the collapsed state at the moment of collapse. At the moment the state collapses $|\omega(t)\rangle$ is Not a finite overlay of coherent states. It was shown that these collapsed field states are of significant significance due to their high non-classical character and may provide a substantial degree of interconnect when they are divided on a vacuum beam splitter at the second input port. In order to investigate the nature of the optical tomogram when the wave packs collapse, we draw the optical tomogram at collapsed time in Eq. $t = T_{rev}/\sqrt{2}$. The optical tomogram is shown in Fig. 4.9 at this moment (d). The sinusoidal strands are not apparent in the optical tomogram for the collapsed state, which means that the optical tomogram of a collapsed state at the moment of fractional reviews is qualitatively different from that of the state. Fig. 4.10 illustrates the starting state's recovery t = T_{rev}. We may infer that in the optical tomogram of time-evolving states signs of revivals and fractional revivals are recorded. At the moment of k-subpacket fractional revivals, the optical tomogram contains k sinusoidal strands for an original coherent state with a strand in the optical tomogram.

References:

1. Bhusal, Narayan. (2021). Smart Quantum Technologies using Photons.
2. Rosas-Ortiz, Oscar & Mendoza, Kevin. (2021). Theory of Photon Subtraction for Two-Mode Entangled Light Beams.
3. Mika, Jaromír & Slodička, Lukáš. (2021). High nonclassical correlations of large-bandwidth photon pairs generated in warm atomic vapor.
4. Kolenderska, Sylwia & Kolenderski, Piotr. (2021). Intensity correlation OCT -- a true classical equivalent of quantum OCT able to achieve up to 2-fold resolution improvement in standard OCT images.
5. Khalil, E. & Mohamed, A.-B.A. & Obada, A. & Elagan, S.K.. (2021). Nonlinear optical tomography of q-deformed entangled pair coherent states. Results in Physics. 20. 103720. 10.1016/j.rinp.2020.103720.
6. Korotkova, Olga & Gbur, Greg. (2020). Applications of Optical Coherence Theory. 10.1016/bs.po.2019.11.004.
7. Swain, Manoranjan & Rai, Amit. (2020). Non classical light in Jx photonic lattice.
8. Olivares, Stefano & Allevi, Alessia & Bondani, Maria. (2020). On the role of the local oscillator intensity in optical homodyne-like tomography. Physics Letters A. 384. 126354. 10.1016/j.physleta.2020.126354.
9. Kolenderska, Sylwia & Vanholsbeeck, F. & Kolenderski, Piotr. (2020). Quantum-inspired detection for Spectral Domain Optical Coherence Tomography. Optics Letters. 45. 10.1364/OL.393162.
10. Lamprou, Theocharis & Liontos, Ioannis & Papadakis, N. & Tzallas, Paris. (2020). A perspective on high photon flux nonclassical light and applications in nonlinear optics. High Power Laser Science and Engineering. 8. 10.1017/hpl.2020.44.
11. Kolenderska, Sylwia & Vanholsbeeck, F. & Kolenderski, Piotr. (2020). Quantum-inspired detection for Spectral Domain Optical Coherence Tomography.